PCCP

Accepted Manuscript

ROYAL SOCIETY OF CHEMISTRY

www.rsc.org/pccp

Journal Name

RSCPublishing

ARTICLE

The Network Simulation Method: a useful tool for locating the kinetic-thermodynamic switching point in complex kinetic schemes

Manuel Caravaca,*[a] Pilar Sanchez-Andrada,*[a] Antonio Soto,[a] and Mateo Alajarin[b].

Cite this: DOI: 10.1039/x0xx00000x

Received 00th January 2012,
Accepted 00th January 2012

DOI: 10.1039/x0xx00000x

www.rsc.org/

The kinetic-thermodynamic switching point of a multistep process, whose reaction mechanism has been elucidated by DFT calculations, can be calculated by means of an efficient model based on the Network Simulation Method (NSM). This method can solve, fast and effectively, a difficult system of differential equations derived from a complex kinetic scheme by establishing a formal equivalence between the chemical system and an electrical network. The NSM employs very short simulation times to determine the dependence of the switching time on the temperature, a fundamental topic to take control over the product composition which has not been treated exhaustively so far, and that could be applied for synthetic purposes avoiding laborious and costly experimental trials.

TOC GRAPHIC

Fast and effective location of the switch point between kinetic and thermodynamic regimes by means of the NSM approach provides a comprehensive control over the product composition

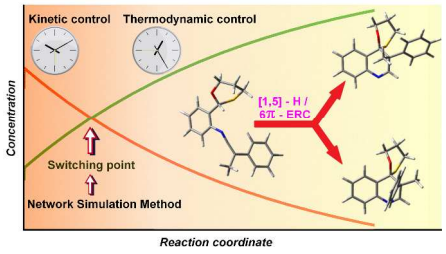

Journal Name RSCPublishing

ARTICLE

I. Introduction

The concept of kinetic versus thermodynamic control is a well settled principle in Chemistry.[1] When a reaction can lead to two or more products from the same reactants, each one of the respective processes follows a particular reaction coordinate. If one product (e. g. **A**) has a lower energy than the second one (e. g. B) but the transition state leading to **A** is higher in energy than that leading to **B**, then **A** and **B** are respectively known as the thermodynamically- and kinetically-controlled products (see Figure 1).

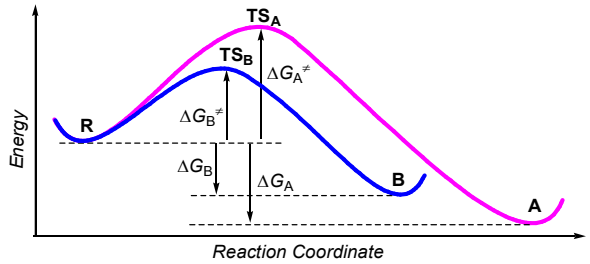

Figure 1. Energy *vs*. reaction coordinate showing the thermodynamically and the kinetically controlled products **A** and **B** respectively.

As it is well-known, the preferential formation of one of these two reaction products, **A** or **B,** can be successfully achieved in some extent by modifying the main variables of the experimental reaction conditions, most usually time and temperature. Thus, running the reaction for long reaction times and at high temperature allows the equilibrium to be reached and consequently the most stable product (**A**) is preferentially obtained over the kinetically-controlled one (**B**). By contrast, short reaction times and low temperatures favor the pathway leading to the faster forming compound **B**, which is habitually isolated as the major component of the product mixture since the reaction is stopped before reaching the equilibrium.

Within this framework, the ability of controlling the composition of the A/B mixture of two reaction products in a particular reaction is of paramount relevance, not only in laboratory organic synthesis but also in important industrial processes. An illustrative example is the kinetically controlled industrial synthesis of semisynthetic antibiotics as amoxicillin, ampicillin, cefadroxil and cephalexin by using penicillin acylase as biocatalyst.[2] Another interesting example is the generation and transformation of nitro-substituted aryl organolitium compounds in microreactors, allowing the preferential formation of the kinetically– or thermodynamically organolitium reagent by changing the residence time.[3]

In spite of the relevance of kinetic *versus* thermodynamic control, the modifications on the time and/or temperature reaction variables usually represent empirical methods of controlling the product composition of chemical processes. In order to achieve a more precise control, we should better be able of calculating the point from which the kinetically-controlled product is no longer the major one in the reaction mixture and the product of thermodynamic control becomes dominant. We define this particular point as the *kinetic-thermodynamic switching point*,[4] characterized in the time scale by a *switching time,* t_s where the concentration of the two reaction products, **A** and **B**, are equal and non-zero (see Figure 2).[5]

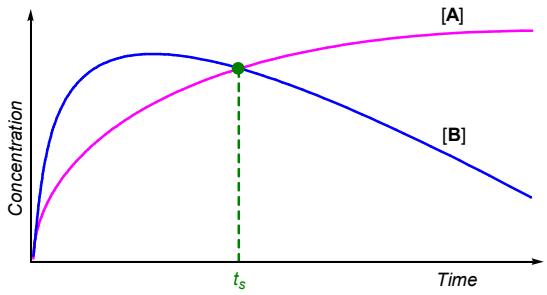

Figure 2. Concentration *vs*. reaction time showing the thermodynamically and the kinetically controlled products **A** and **B** respectively, and the switching point.

It seems conceptually obvious that the switching time should be dependent on the reaction temperature. Shorter switching times would be reached by increasing the reaction temperature and viceversa. Therefore, to deepen into the occurrence of the switching time, we must perform an exhaustive study of this dependence. Besides, in order to determine the concentration of the desired species (**A** or **B**) along the reaction time, it is essential to obtain a graph as that shown in Figure 2 for the process of interest. Now the question is how to calculate it.

Obviously a thorough kinetic study is mandatory, either via a comprehensive experimental work, expensive in terms of time and effort, or by means of theoretical calculations, a more amenable approach. To address the problem under this latter choice, first we must compute the detailed reaction mechanism, including all the stationary points and energy barriers, then write the corresponding kinetic scheme, and finally solve the associated mathematical equations.

Quantum mechanics calculations allow us to explore the potential energy surface associated to the transformation of reactants into products and to elucidate the mechanistic paths connecting them. A lot of information is thus obtained such as the structure of the involved stationary points (minima, intermediates and transition states), its energies, and thereafter the energy barriers of all the individual reaction steps. From these data, by applying the transition state

theory[6] which connects thermodynamic and kinetics, it is also possible to find the kinetic coefficients, *i. e.* the rate constants, associated to each mechanistic step.

Next, kinetic studies at constant volume lead to a system of first order ordinary differential equations, the chemical rate equations, which express the time evolution of the concentration of the chemical species involved in the reaction, *i. e.*, reactants, intermediates, and products.[7] If we call $[\boldsymbol{x_i}]$ the concentration of the *i*-th participant species, the chemical kinetic equation presents the following form:

$$\frac{d\,[\boldsymbol{x_i}]}{dt} = f([\boldsymbol{x_1}], [\boldsymbol{x_2}] \ldots [\boldsymbol{x_n}]) \quad (1)$$

where the derivative of $[\boldsymbol{x_i}]$ is a function of the concentration of all or some of the *n* participant species, which also depends on a specific set of *m* rate constants $\{k_j\}$, $j = 1, m$.

The solution of the corresponding system of differential equations then would reveal the variation over time of the concentrations of all the species at a fixed temperature, thus allowing to locate the precise kinetic-thermodynamic switching point. However, these systems of differential equations are frequently difficult to solve analytically, the degree of difficulty being generally proportional to the complexity of the reaction mechanism (number of intermediates and reaction steps). In fact, in some cases the mechanistic scheme is so complex that it is complicated even to identify which is the kinetically-controlled product from the resulting reaction profiles.

In such complex cases, chemists frequently make use of a series of approaches to simplify calculations.[7,8] These assumptions can sometimes lead to incorrect results and often restrict the validity of the study to certain reaction conditions.

Numerical simulations are effective tools to accomplish the kinetic study,[9] because they do not need, in principle, to make use of approximations in the theoretical model. Nevertheless, when the kinetic scheme is so complex, or several features of the chemical system, such as the switching point or the stationary state, occur at very long times, some of these methods turn into inefficient. Thus, finding a comprehensive, fast and effective numerical approach for solving these cases would be a valuable help.

Here we employ a simple and general approach, the Network Simulation Method (NSM),[10] able to solve any difficult system of differential equations of a complex kinetic scheme, as well as to calculate efficiently the point of kinetic-thermodynamic switch (if exists) even when it occurs at long switching times. Furthermore, this approach allows us to easily predict the concentration of the participant species as a function of time, even at low temperatures, where very long reaction times can be necessary to reach the stationary state.

Remarkably, the NSM establishes a formal equivalence between the chemical transport processes and electrical networks, which could be applicable to any complex kinetic scheme without using any theoretical approximation. To this end, a software of circuit analysis such as Pspice,[11] in which the NSM is implemented, has to be employed. Its reliability and quickness make this smart method a convenient choice for accurately studying these systems.

It is also worth pointing out that our results show that the NSM could be even orders of magnitude faster than the standard simulation algorithms employed to solve ordinary differential equations, such as fourth order Runge-Kutta and others.[12]

To illustrate how the NSM can be applied to solve the issues raised in this work, we will first present the method and its application to the simplest mechanistic scheme, considered above, **A** ⇄ **R** ⇄ **B** (Figure 1), by calculating its kinetic-thermodynamic switching point. Then, by examining a particular case entailing a mechanism of higher complexity, we will present the complete protocol to follow, from the elucidation of the reaction mechanism to the resolution of the system of kinetic differential equations and the location of the kinetic-thermodynamic switching point.

II. The Network Simulation Method

The Network Simulation Method is a numerical approach which establishes an analogy between a set of differential equations and an electric network model. The origin of this methodology comes from the early seventies with the study of thermodynamic systems by means of the so called *network thermodynamics*[13] However, today their applications are still under study, and it has been applied successfully to solve strongly nonlinear problems in such diverse fields as heat transfer[14], chemical diffusion-reaction systems[15], groundwater flow[16], inverse problems[17], ecological systems[18] and elastic waves in materials.[19]

The electrical analogy of the kinetic chemical problems has been addressed previously. Mikulecky et al. modelled the cellular folate metabolism scheme,[20] which plays an important role in cancer chemotherapy. However, the electrical analogy applied to kinetic systems is still a matter of study.[21]

To specifically solve a kinetic chemical scheme by applying the NSM method it is first mandatory to design the equivalent network model for the system of differential equations, and then simulate the circuit by means of suitable electric circuit analysis software such as Pspice.

Two steps have to be followed to design a circuit network. First of all, an independent electric circuit is assigned to each differential equation of the mathematical model, which will be connected with the other circuits by means of a common node. The whole problem is thus established as a global electric network containing as many circuits as equations. Each addend inside each differential equation is considered as a current branch which converges into an appropriated node, in which Kirchhoff´s current law (KCL) is satisfied.[10] The electrical analogy establishes that the voltage of this

node is exactly the concentration of the compound whose concentration varies along time.

For convenience, we can rewrite eq. 1 in the KCL form:

$$\frac{d\,[\boldsymbol{x_i}]}{dt} - f([\boldsymbol{x_1}], [\boldsymbol{x_2}] \ldots [\boldsymbol{x_n}]) = 0 \quad (1')$$

Due to the mathematical signs of the addends inside each equation, their associated currents will be of two types: incoming current branches (negative sign) and outgoing current branches (positive sign), thus satisfying the KCL.

Each current branch of the network is implemented by a particular and appropriate electrical device. The main problem is how to assign them to each term inside the differential equations. Furthermore, these equations will usually be coupled, so the problem increases in complexity. This last fact implies that an individual circuit, which models one particular differential equation, could present current branches that are functions of any node voltages of the electrical network (for further details see Supporting Information).

In general, there are three kind of devices employed to design each electric circuit (see Table 1):[10]

(i) One capacitor, associated to the species whose time derivative of its concentration appears in the differential equation ($d[\boldsymbol{x_i}]/dt$ in eq. 1'). The current I_c at the ends of a capacitor is $I_c = C\, dV/dt$, which can be directly related to the first derivative of the concentration. Since the derivative in eq. 1' has a positive sign, the corresponding current branch will be outgoing from the corresponding voltage node of the circuit.

(*ii*) Voltage-controlled current sources, one per addend inside each differential equation, excluding $d[\boldsymbol{x_i}]/dt$. This kind of device is a current source whose value can be defined as a function of other voltages of the network. So, it allows the implementation of the coupled terms inside the differential equation. Its associated branch current can be either incoming or outgoing from the circuit voltage node, depending on the sign of the addend.

(*iii*) A resistor of high value, a device that does not model any term of the differential equations, but it is necessary to guarantee criteria of continuity.

Once the network model is completed, its simulation is carried out by Pspice, which makes use of the sophisticated numerical techniques of analysis that these kinds of codes embody.[22] It is important to stand out that mathematical manipulations inherent to this kind of numerical problems, such as numerical algorithms, output data organization, convergence criteria, among others, as well as additional requirements, such as those referring to mass conservation equations, are not necessary in this method since the chosen software performs this work.

Finally, the initial conditions are implemented by fixing the voltage of the condensers.

a. Illustrative application of the NSM to a prototypical reaction

The simplest mechanistic scheme where we can calculate the kinetic-thermodynamic switching point to illustrate the NSM is that corresponding to the reaction profile depicted in Scheme 1,[23] a unimolecular reaction where the reactant **R** evolves to the product **A** and **B**. This corresponds to the following kinetic scheme:

Scheme 1. Mechanistic scheme for the transformation of reactant **R** into the products **A** and **B** showing the rate constants of each process.

The corresponding kinetic study involves three differential equations, eqs. (2)-(4), so three independent (electrically isolated) circuits (as those shown in Figure 3) will appear in the network model of the cell.

$$\frac{d[\mathbf{R}]}{dt} = -(k_a + k_b)[\mathbf{R}] + k_{-a}[\mathbf{A}] + k_{-b}[\mathbf{B}] \quad (2)$$

$$\frac{d[\mathbf{A}]}{dt} = k_a[\mathbf{R}] - k_{-a}[\mathbf{A}] \quad (3)$$

$$\frac{d[\mathbf{B}]}{dt} = k_b[\mathbf{R}] - k_{-b}[\mathbf{B}] \quad (4)$$

In this particular case, the system of coupled differential equations can be analytically solved.[24]

For simplicity, as a representative example we will focus on equation (2), which involves the variation of species **R** with time, which can be rewritten as follows in order to resemble Kirchhoff's current law:

$$\frac{d[\mathbf{R}]}{dt} + (k_a + k_b)[\mathbf{R}] - k_{-a}[\mathbf{A}] - k_{-b}[\mathbf{B}] = 0 \quad (5)$$

This equation can be implemented by a four branches circuit plus a resistor of very high value, as can be seen in the top circuit of Figure 3. Each addend is considered as a transport variable, i. e., concentration flow which is balanced with the rest of the terms according to their algebraic sign at the node **R**. The voltage at the node **R** or, equivalently, the voltage at the capacitor, is the value of the variable [**R**]. The capacitor is denoted as $C_{\mathbf{R}}$. According to the form of the term $d[\boldsymbol{R}]/dt$, we set the value of the capacitor equal to 1 F (see Supporting Information). The rest of the addends are easily implemented by the voltage-controlled current sources. So, the addend (k_a+k_b) [**R**] is modelled by a current source $G_{\mathbf{R}_1}$, whose explicit form is defined in Pspice as a function of k_a, k_b and [**R**]. The same procedure is applied for implementing the addends $-k_{-a}\cdot$[**A**] and $-k_{-b}\cdot$[**B**], respectively, with sources $G_{\mathbf{R}_2}$ and $G_{\mathbf{R}_3}$, respectively (see Table 1).

Table 1. Electrical Modelling Implementation of Each Term of the KCL Form of the Differential Equation[a]

$$\frac{d[\mathbf{R}]}{dt} + (k_a + k_b)[\mathbf{R}] - k_{-a}[\mathbf{A}] - k_{-b}[\mathbf{B}] = 0$$

Terms	Electrical Devices	
$\frac{d[\mathbf{R}]}{dt}$	Capacitor $C_{\mathbf{R}}$ (1 F) (outgoing current branch)	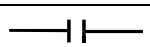
$(k_a + k_b)[\mathbf{R}]$	Voltage-controlled current source $G_{\mathbf{R}_1}$ (outgoing current branch)	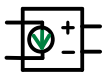
$-k_{-a}[\mathbf{A}]$	Voltage-controlled current source $G_{\mathbf{R}_2}$ (incoming current branch)	
$-k_{-b}[\mathbf{B}]$	Voltage-controlled current source $G_{\mathbf{R}_3}$ (incoming current branch)	

[a] The sign of the addends of the differential equation is modelled by changing the polarity of the Voltage-controlled current source.

We must perform this overall process for each differential equation, which will be modelled as a circuit containing as many branches in parallel as addends in the equation. Thus, the whole problem is equivalent to a global electric network containing three main circuits (see Figure 3) of two nodes each one: a common node (the circuit ground) and an independent node whose voltage is the unknown variable, *i. e.*, the concentration of the chemical species.

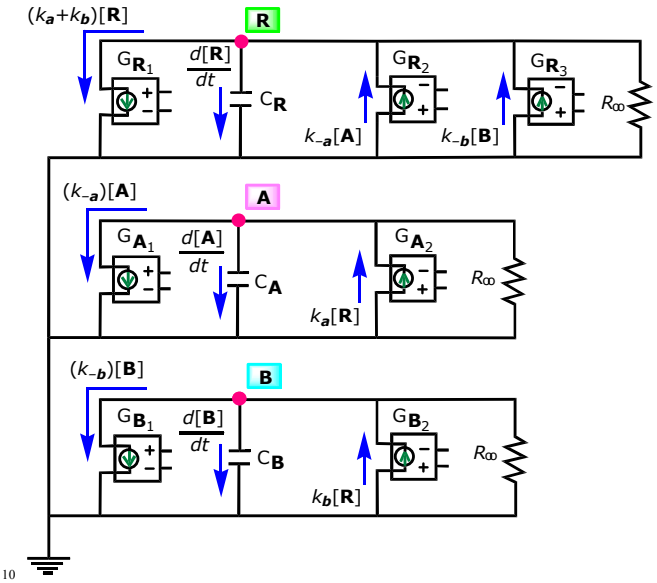

Figure 3. Network model designed for the kinetic scheme of the transformation of **R** into **A** and **B** according to the one-step mechanism **A** ⇄ **R** ⇄ **B**

The results obtained from the implementation of the network model of Figure 3 in Pspice are shown in Figure 4, where the concentration of species **A** and **B** *versus* time are plotted. Arbitrary values of the rate constants (k_a = 691.61, k_b = 396.16, k_{-a} = 0.37 and k_{-b} = 0.02, in s^{-1}), and the following initial conditions: $[\mathbf{R}]_0$ = 1 mol/l; $[\mathbf{A}]_0 = [\mathbf{B}]_0$ = 0 mol/l have been chosen. From the simulation, the kinetic-thermodynamic switching point was easily determined. From figure 4 it can be inferred that the switching time is equal to 1.94 seconds.

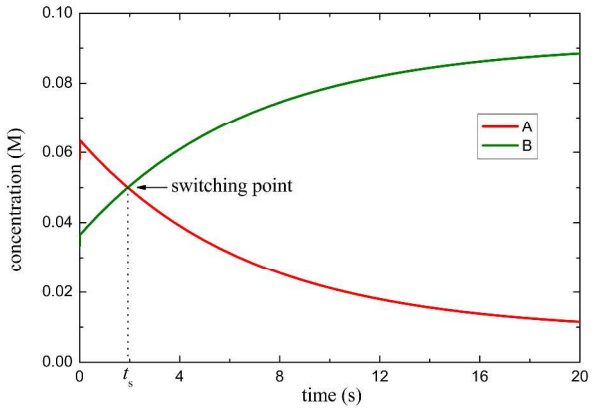

Figure 4. Plot of concentration of the kinetically and thermodynamically controlled products **A** and **B** versus the reaction time showing the switching point for the transformation **A** ⇄ **R** ⇄ **B**.

III. The NSM applied to a tandem of pericyclic processes

Now, we are in disposition to explain how to solve a more complex system with the NSM.

Recently, some of us have disclosed an experimental and theoretical study on the conversion of ketenimines bearing 1,3-oxathiane (**1**) units into the diastomeric spiro-1,3-oxathianequinolines (**2**) depicted in Scheme 2.[25]

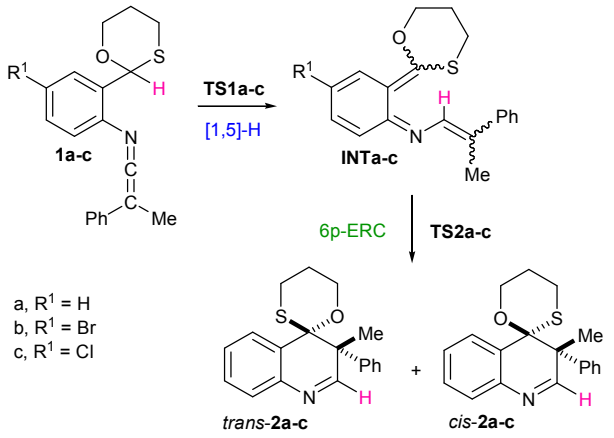

Scheme 2. The two reaction steps for the conversion of oxathiane-ketenimines **1** into the spiroquinolines **2**.

The computational assessment of the conversion **1a**→**2a**, allowed us to elucidate the mechanistic paths of these transformations: two consecutive pericyclic processes

consisting of a [1,5]-H shift of the acetalic hydrogen atom, followed by a 6π-electrocyclic ring closure.

Interestingly, the initial [1,5]-H shift, causes the generation of two stereogenic double bonds and, consequently, four isomeric *o*-azaxylylene intermediates, ***E,E*-INTa**, ***E,Z*-INTa**, ***Z,E*-INTa** and ***Z,Z*-INTa** can be formed via the corresponding isomeric transition structures (***E,E*-**, ***E,Z*-**, ***Z,E*-**, ***Z,Z*-TS1a**). Each of these four intermediates undergoes a 6π-electrocyclic closure leading to the diastereomeric spiroquinolines *trans*-**2a** or *cis*-**2a** according to the reaction paths disclosed in Scheme 3. The spirocompound *trans*-**2a** is slightly higher in energy than *cis*-**2a**, and therefore, the latter was predicted to be the thermodynamically controlled product.

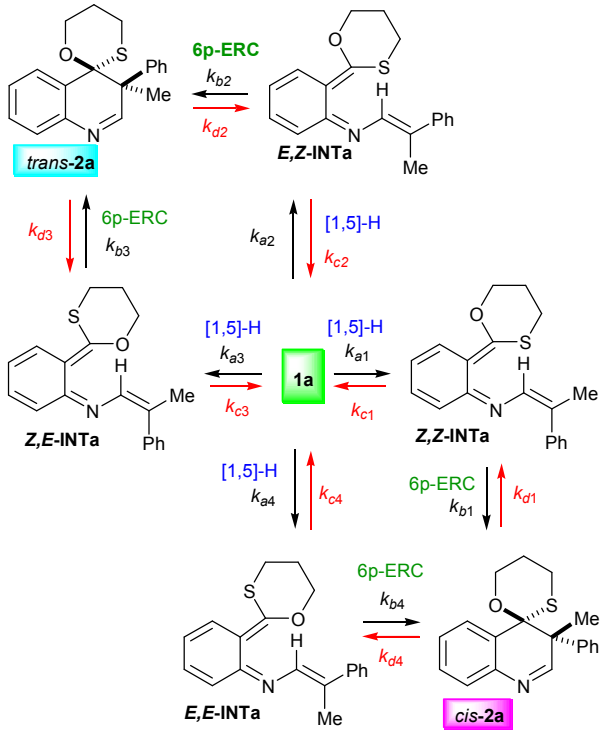

Scheme 3. Mechanistic paths from the computational study for the conversion of 1,3-oxathiane-ketenimine **1a** into *cis*- and *trans*-spiroquinolines **2a** showing the rate constants corresponding to each step.

By examining the resulting reaction profiles and the energy barriers associated to each step it was impossible to distinguish which of the two final species (*cis*- or *trans*-**2a**), is the kinetically controlled product.[26] To rationalize the stereocontrol degree obtained in the experimental work, we then calculated the ratio of spiroquinolines *cis*-**2a**/*trans*-**2a** by carrying out a quantitative kinetic analysis and solving analytically the resulting system of differential equations.[27] To this end we used two assumptions: on the one hand we applied the Steady State Approximation (SSA) and on the other hand, we considered irreversible the conversion of the intermediates into the final spiroquinolines. This last guess was made on the basis of the low values of the corresponding rate constants when compared with those associated to the rest of processes, $k_{d1\text{-}4} << k_{a1\text{-}4}$, $k_{b1\text{-}4}$, $k_{c1\text{-}4}$.[28] Therefore, and taking into account that *cis*-**2a** is lower in energy than *trans*-**2a**, we assumed the reaction under kinetic control.

Accordingly, we obtained the following solutions for [**1a**], [*cis*-**2a**] and [*trans*-**2a**], as well as for the ratio [*cis*-**2a**]/[*trans*-**2a**], which is a combination of the considered rate constants, and independent of the reaction time:[29]

$$[\mathbf{1a}] = e^{\alpha t} \qquad (6)$$

$$[cis-\mathbf{2a}] = \left(\frac{\beta}{\alpha}\right)[e^{\alpha t}-1] \qquad (7)$$

$$[trans-\mathbf{2a}] = \left(\frac{\gamma}{\alpha}\right)[e^{\alpha t}-1] \qquad (8)$$

$$\frac{[cis-\mathbf{2a}]}{[trans-\mathbf{2a}]} = \left\{\frac{\left[\left(\frac{k_{a1}\cdot k_{b1}}{k_{b1}+k_{c1}}\right)+\left(\frac{k_{a4}\cdot k_{b4}}{k_{b4}+k_{c4}}\right)\right]}{\left[\left(\frac{k_{a2}\cdot k_{b2}}{k_{b2}+k_{c2}}\right)+\left(\frac{k_{a3}\cdot k_{b3}}{k_{b3}+k_{c3}}\right)\right]}\right\} \qquad (9)$$

With $k_i = \frac{K_B\cdot T}{h}\cdot e^{\frac{\Delta G_i}{RT}}$ (10)

where α, β, and γ are functions of the rate constants, and t is the reaction time in seconds. From eq. (9) we calculated a ratio [*cis*-**2a**] / [*trans*-**2a**] of 0.49 at 410 K (the temperature employed in the experimental work), quite approximated to those obtained experimentally.[25]

These results were satisfactory because we could carry out a complex kinetic study allowing us to predict the reaction products ratio, and establish that *trans*-**2a** and *cis*-**2a** are respectively the kinetically and thermodynamically controlled products. Nevertheless, these solutions, eqs. (6)-(9), are only valid for short reaction times. Moreover, from this approach, given that the second steps were considered irreversible, it is impossible to reach thermodynamic equilibrium, and consequently the switching point does not occur.

Furthermore, despite the concordance between experimental and theoretical results, some general questions cannot be answered due to the limitations imposed by the approximations made:

Is it possible to determine the dependence of the switching time on temperature in such a complex system? Is the employed reaction time adequate for obtaining the maximal reaction yield? Is one of the species both the kinetically and thermodynamically controlled product (no switching point)? Or, by contrast, one species is the kinetically controlled product and the other is the thermodynamically one? The application of the NSM leads to an accurate answer for each of these questions.

a. Mathematical Model

The mechanism depicted in Scheme 3 can be modelled by the following system of first order ordinary differential equations:

$$\frac{d[\mathbf{1a}]}{dt} = -(k_{a1} + k_{a2} + k_{a3} + k_{a4})[\mathbf{1}a] + k_{a1}[\boldsymbol{Z},\boldsymbol{Z} - \mathbf{INT}\boldsymbol{a}] + k_{a2}[\boldsymbol{E},\boldsymbol{Z} - \mathbf{INT}\boldsymbol{a}] + k_{a3}[\boldsymbol{Z},\boldsymbol{E} - \mathbf{INT}\boldsymbol{a}] + k_{a4}[\boldsymbol{E},\boldsymbol{E} - \mathbf{INT}\boldsymbol{a}] \quad (11)$$

$$\frac{d[\boldsymbol{Z},\boldsymbol{Z} - \mathbf{INT}\boldsymbol{a}]}{dt} = k_{a1}[\mathbf{1a}] - (k_{b1} + k_{c1})[\boldsymbol{Z},\boldsymbol{Z} - \mathbf{INT}\boldsymbol{a}] + k_{d1}[cis - \mathbf{2a}] \quad (12)$$

$$\frac{d[\boldsymbol{E},\boldsymbol{Z} - \mathbf{INT}\boldsymbol{a}]}{dt} = k_{a2}[\mathbf{1a}] - (k_{b2} + k_{c2})[\boldsymbol{E},\boldsymbol{Z} - \mathbf{INT}\boldsymbol{a}] + k_{d2}[trans - \mathbf{2a}] \quad (13)$$

$$\frac{d[\boldsymbol{Z},\boldsymbol{E} - \mathbf{INT}\boldsymbol{a}]}{dt} = k_{a3}[\mathbf{1a}] - (k_{b3} + k_{c3})[\boldsymbol{Z},\boldsymbol{E} - \mathbf{INT}\boldsymbol{a}] + k_{d3}[trans - \mathbf{2a}] \quad (14)$$

$$\frac{d[\boldsymbol{E},\boldsymbol{E} - \mathbf{INT}\boldsymbol{a}]}{dt} = k_{a4}[\mathbf{1a}] - (k_{b4} + k_{c4})[\boldsymbol{E},\boldsymbol{E} - \mathbf{INT}\boldsymbol{a}] + k_{d4}[cis - \mathbf{2a}] \quad (15)$$

$$\frac{d[cis - \mathbf{2a}]}{dt} = k_{b1}[\boldsymbol{Z},\boldsymbol{Z} - \mathbf{INT}\boldsymbol{a}] + k_{b4}[\boldsymbol{E},\boldsymbol{E} - \mathbf{INT}\boldsymbol{a}] - (k_{d1} + k_{d4})[cis - \mathbf{2a}] \quad (16)$$

$$\frac{d[trans - \mathbf{2a}]}{dt} = k_{b2}[\boldsymbol{E},\boldsymbol{Z} - \mathbf{INT}\boldsymbol{a}] + k_{b3}[\boldsymbol{Z},\boldsymbol{E} - \mathbf{INT}\boldsymbol{a}] - (k_{d2} + k_{d3})[trans - \mathbf{2a}] \quad (17)$$

The mathematical model is completed by assuming the following initial conditions:

$[\mathbf{1a}]_0$ = 1 mol/L;

$[\boldsymbol{Z},\boldsymbol{Z}\text{-}\mathbf{INTa}]_0 = [\boldsymbol{E},\boldsymbol{Z}\text{-}\mathbf{INTa}]_0 = [\boldsymbol{Z},\boldsymbol{E}\text{-}\mathbf{INTa}]_0 = [\boldsymbol{E},\boldsymbol{E}\text{-}\mathbf{INTa}]_0 = [cis\text{-}\mathbf{2a}]_0$, $= [trans\text{-}\mathbf{2a}]_0 = 0$, where the subscript 0 refers to time t=0.

IV. Results and Discussion

The numerical analysis of the set of coupled differential equations (11)-(17) was carried out, as shown in the previous section, through the application of the Network Simulation Method by means of Pspice.

By operating in the same way as shown in the illustrative example presented above, the total system will be equivalent to a global electric network containing seven main circuits of two nodes each one, as depicted in Figure 5.

Journal Name RSCPublishing

ARTICLE

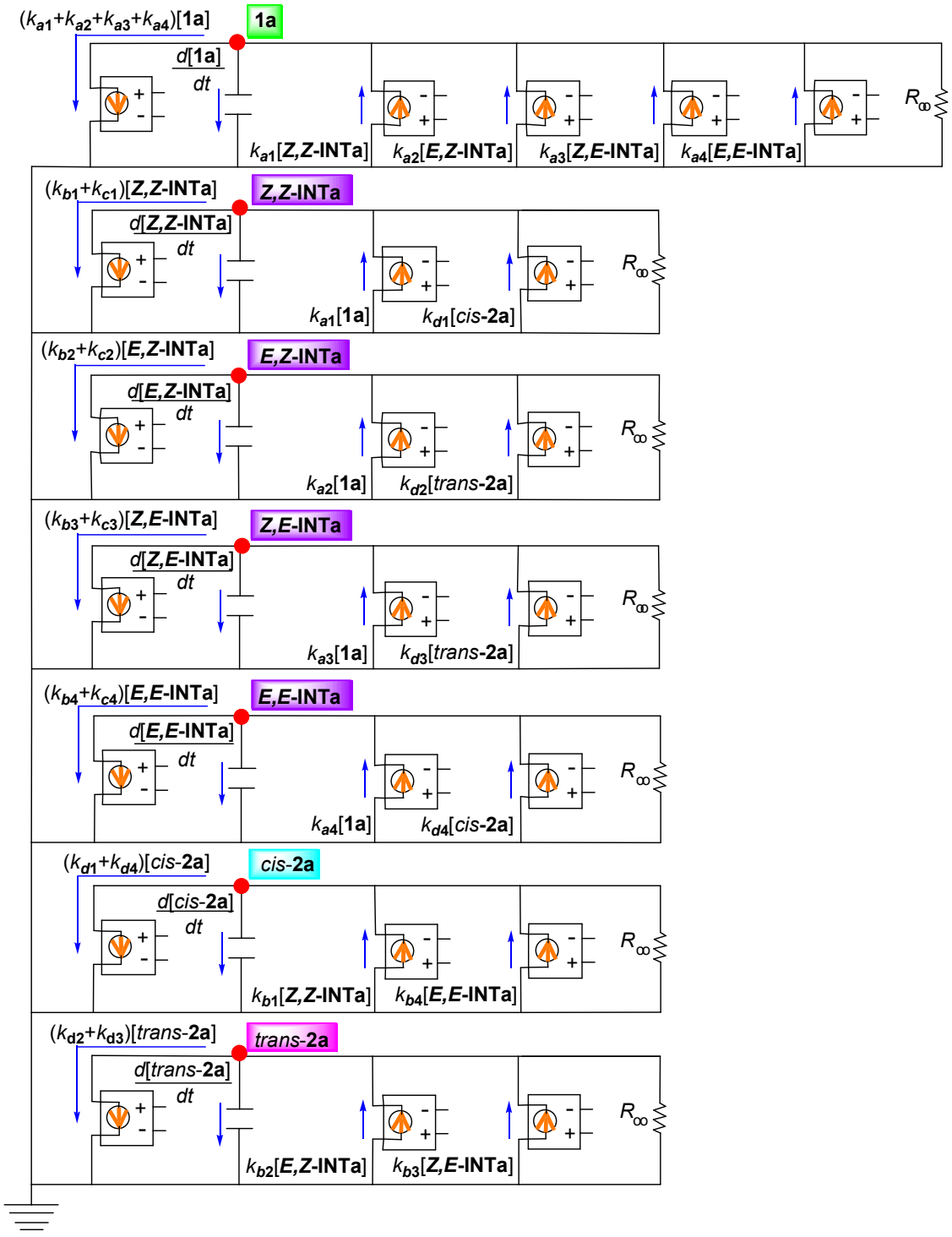

Figure 5. General network model equivalent to equations (11)-(17) corresponding to the kinetic scheme for the transformation of 1,3-oxathiane-ketenimine **1a** into *cis*- and *trans*-spiroquinolines **2a**.

Journal Name RSCPublishing

ARTICLE

We have considered different temperature values, *T,* ranging from 320 to 500 K. In this way, we are presumably working in in the appropriate temperature range to allow the desired reaction to take place and, simultaneously, to minimize side reactions. To this end, the energy barriers corresponding to each step involved in the transformation of **1a** into *cis*-**2a** and *trans*-**2a** were computed at different temperatures at the B3LYP/6-31+G** theoretical level in Gaussian09,[30] and then the sets of rate constants ($k_{a1\text{-}4}$, $k_{b1\text{-}4}$, $k_{c1\text{-}4}$, $k_{d1\text{-}4}$,) were calculated. In order to save space in the MS these sets of values are shown in Table S2 of the Supporting Info.

The results obtained for all temperatures are qualitatively the same, hence, with the aim to compare them with those obtained in reference 25, we will firstly focus on those corresponding to T=410 K. Thereafter, we will analyze the influence of the temperature in the switching time.

In Figure 6 we represent the concentration of the spiroquinolines *cis*-**2a** (black curves) and *trans*-**2a** (red curves), the thermodynamically and kinetically controlled products, respectively, as a function of time for T=410 K. The continuous curves correspond to the data obtained from the NSM, while the dashed curves are plots of eqs. (7) and (8) corresponding to the analytical solution previously calculated. It is important to realize, by comparing the solid and dashed curves, that theoretical solution does not differentiate between the kinetic regime, where the concentration of product *cis*-**2a** goes below that of product *trans*-**2a,** and the thermodynamic one, where the concentration of *cis*-**2a** goes above that of product *trans*-**2a**. However, the continuous curves clearly show the change of regime, which is characterized by a cutoff time, the so called switching time, t_s. It can only be observed when the second steps, the electrocyclic ring closure processes shown in Scheme 3, are considered reversible. For that purpose, it is necessary to include in the kinetic study the corresponding rate constants $k_{d1\text{-}4}$. From data of Figure 6 we can determine that the switching time is $t_s = 2.16 \cdot 10^7$ s for T=410 K.

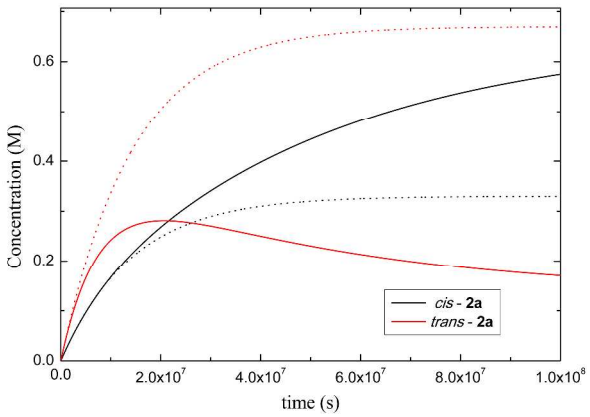

Figure 6. Dependence of concentrations [*cis*-**2a**] (black curves) and [*trans*-**2a**] (M) (red curves) on the reaction time (s) for T=410 K. Solid lines correspond to results calculated from the NSM and reveal the thermodynamic-kinetic switch, while dashed lines are those obtained from equations (7) and (8).

We can also note that the time for both species to reach the stationary state is greater when we consider all reverse step processes. In fact, the dashed lines are roughly constant from $t=1.0 \cdot 10^8$ s, while the solid ones need greater times to reach the stationary regime.[31]

Despite the apparent discrepancies, the dashed and solid curves match at sufficiently short times. To show this, in Figure 7 we represent a detail of Figure 6 until $t=5.0 \cdot 10^5$ s, which is within the typical time range employed experimentally for these pericyclic reactions. To distinguish between data that comes from the previous theoretical approach and from our numerical simulations, at short times, we have replaced the dashed lines shown in Figure 7 by dots. From the plot we can determine that the curves match until a time close to $2.0 \cdot 10^5$ s, from which they start to diverge. This result reveals two important facts regarding the two approximations made in reference 25: (a) the application of the steady-state approximation to intermediates ***E*,*E*-INTa**, ***E*,*Z*-INTa**, ***Z*,*E*-INTa** and ***Z*,*Z*-INTa** remains valid. To show this, in our numerical study we have checked that the concentrations of these intermediates are approximately constant and close to zero, not only at short times, but over the entire time range of simulation (see Figure S2 in the Supporting Information); (b) in relation to the irreversibility of the second steps (electrocyclizations of intermediates into the final spiroquinolines), we can conclude that these back step processes can be reasonably neglected at short times, as those shown in Figure 7.

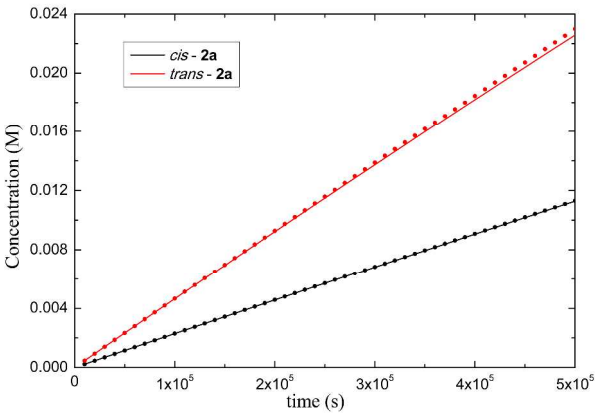

Figure 7. Detail of Figure 6 at short times showing the dependence of concentrations [*cis*-**2a**] (black) and [*trans*-**2a**] (red) (M) on the reaction time (s) for *T*=410 K, obtained from the NSM (solid curves) and from equations (7) and (8) (dots).

Let us discuss in more detail this last assumption. It is a known fact that the rate-limiting step (RSL) is the slowest step in a series of chemical reactions, which sets the overall rate of the multi-step reaction, and generally is that requiring the greatest activation energy. In consecutive organic reactions, it is usual to find great differences between the individual rate steps, so when we determine the rate of the overall process, we are actually measuring the rate of the RSL. This statement can be easily understood in terms of probability. In our study, these rate constants k have units of frequency (s^{-1}), which implies that the corresponding step takes place "k times per second", or equivalent, that the related process occurs once every "$1/k$" seconds. It is clear from this argument that the reaction time required to achieve the balanced regime must be greater than "$1/k^*$", where k^* is the rate constant corresponding to the RSL.

The ratio *cis*-**2a**/*trans*-**2a** obtained in ref. 25 was determined for $t=6\cdot10^4$ s and T=410 K. At that temperature, the rate constant of the RSL, which is the slowest of the reverse processes of the second steps, is $k_{d4}=2.05649\cdot10^{-9}$ s^{-1}. Besides, rate constants k_{d1-3} are still very small when compared with the rest of the set $\{k_j\}$ (see Table S4). This fact clearly shows that at very short times was appropriated to disregard these reverse processes, as done in the theoretical approach previously reported.

Moreover, at this point it should be noted, that when the value of the RSL rate constant is very small, the switching time (if the switching point exists) is expected to be very high, and therefore, traditional simulation algorithms become inefficient given the high CPU time consumed (see below).

As commented above, in reference 25 some of us calculated that the ratio [*cis*-**2a**]/[*trans*-**2a**] was 0.49, obtained by employing eq. (9), which was time independent. Actually, this ratio is an increasing function of time until the stationary state is reached, where it becomes a constant. We plotted in Figure 8 the ratio of species *cis*-**2a** and *trans*-**2a** extracted from our simulations, versus the reaction time.[32] We can conclude that, in effect, the ratio of both species is not constant and its behavior is roughly linear in a small time range, until $t=5.0\cdot10^5$ s, as it can be observed in the detail of the plot. For $t=3.2\cdot10^4$ s we have determined that the ratio is equal to 0.49, in agreement with the previous work.[25]

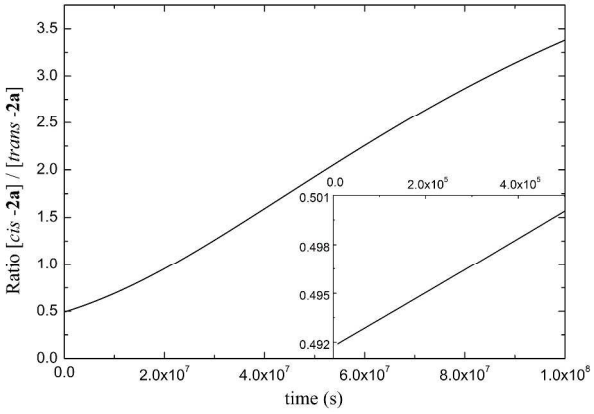

Figure 8. Ratio [*cis*-**2a**] / [*trans*-**2a**] *vs.* the reaction time (s) calculated from the NSM at *T*=410 K.

The reaction yield is another interesting variable we can predict directly from our calculations. It can be easily monitored by measuring the amount of product obtained in the reaction as a function of time. [33]

Equation (6) predicts that the concentration of the reactant, **1a,** tends to zero at very long times, so the reaction yield gets a stationary value of 100%. Our simulations reveal, as can be seen in Figure 9, that the reaction yield is a monotonically increasing function of time up to $t=2.0\cdot10^8$ s. The curve gets into a stationary regime from a time close to $3.0\cdot10^8$ s, but reaches a constant value equal to 78.5%. This result may seem surprising, since these data show that the reaction yield will not reach 100%, but it is due to the fact that the concentration of **1a** does not tend to zero as the steady state is reached. In fact, from these simulations we have determined that in the stationary state the concentration of **1a** is stabilized at a constant value of 0.22 M at 410 K (see Figure S4 in Supporting Info). In the detail of Figure 9 we can observe that the behavior of the reaction yield is roughly linear until a time close to $1.0\cdot10^5$ s. This latter plot is relevant because indicates how to improve the reaction yield by only controlling the experimental reaction time.

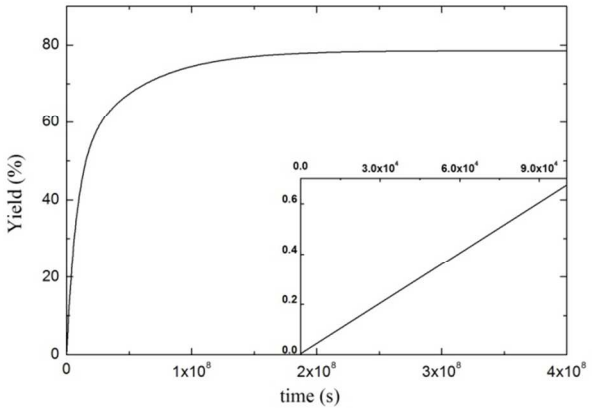

Figure 9. Dependence of the reaction yield (%) on the reaction time (s) obtained from the NSM on the transformation of **1a** into *cis*-**2a** + *trans*-**2a** at *T*=410 K.

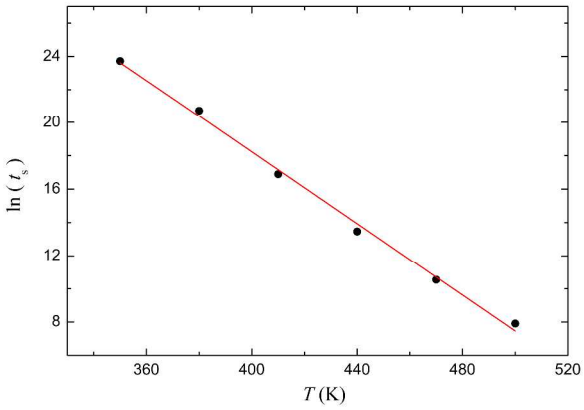

Figure 10. Natural logarithm of the thermodynamic-kinetic switch time, t_s (time in seconds) *vs* temperature, *T* (K), obtained for the transformation of **1a** into *cis*-**2a** + *trans*-**2a** from NSM.

To complete the study of the reaction yield, we have also computed the dependence of this variable on the reaction time but considering irreversible the second steps shown in Scheme 3 (*i. e.*, the 6π-electrocyclic ring closures). The results indicated that the yield reaches a constant value equal to 100% from a proper time of $1.0 \cdot 10^8$ s (see Figure S5 in Supporting Info). This outcome is consistent with the fact that, within this scenario, the concentration of compound **1a** tends to zero as the steady situation is achieved.

The occurrence of the kinetic-thermodynamic switching point is a fundamental task in our numerical study. In order to achieve a deeper comprehension of the phenomenon, we need to quantify the influence of the temperature on the switching point. Finding an explicit dependence of t_s on *T* allows us to take control over the change of regime. For the new simulations, the appropriated set of rate constants $\{k_i\}$ has been chosen (see Table S4 in Supporting Information).[34] It is worth to point out that is the variable time, not the temperature, the factor that controls the kinetic-thermodynamic switching point. The temperature only affects the position of the switching time t_s.[35] This assumption can be inferred from the simulations at different temperatures. In Figure 10 a plot of the natural logarithm of t_s *vs.* *T* (dots) and the linear fit of the curve (solid line) are disclosed. The fit reveals that t_s has a good exponential behavior in terms of *T* as can be stated form the correlation coefficient *r,* which is equal to -0.996. The fitted expression for $\ln(t_s)$ is:

$$\ln(t_s) = -0.11T + 61.31$$

which constitutes a suitable formula for determining t_s as a function of *T* in the operating temperature range described in this work.

To conclude, we have carried out other numerical approaches to estimate the validity and consistency of the Network Simulation Method in this study. Specifically, we applied the fourth-order Runge-Kutta (RKM)[36] and the Bulirsch-Stoer (BS)[12] algorithms, both computed in Fortran. The Runge-Kutta method is a standard procedure in numerical analysis to solve ordinary differential equations and the Bulirsch-Stoer is an improved adaptive method designed for the same proposal, which presents a high accuracy with relatively little computational effort. We have obtained identical results from the application of these two algorithms to the set of equations (11)-(17). Furthermore, the representation of concentration versus time for all species match with that obtained from the NSM in Pspice, over the entire time range. In Figure 11 the concentrations of species *cis*-**2a** (black) and *trans*-**2a** (red) from the NSM (solid curves) and from the fourth-order Runge-Kutta method (dots) are depicted. We conclude that both methods give the same numerical results.

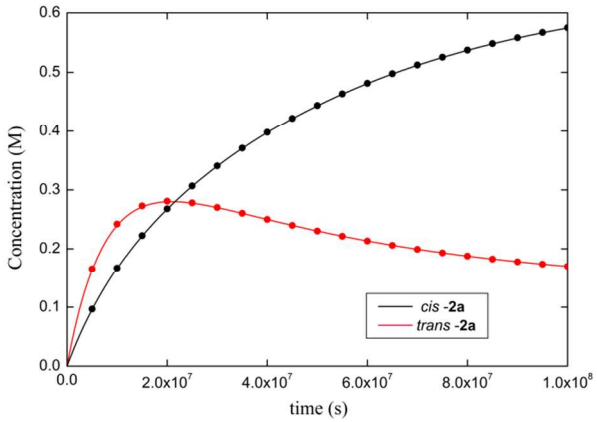

Figure 11. Comparison of the NSM (solid curves) and the RKM (dots) applied to the calculation of concentrations [*cis*-**2a**] (red) and [*trans*-**2a**] (black) as a function of the reaction time (s), for *T*=410 K.

The major problem arising from the application of the RKM to our set of kinetic differential equations is the choice of the discretized step, the so called step-size control.[37] Generally, when employing a programming language as Fortran, it's necessary to take control over all the variables in the program, which requires special skills in manipulating the code. In our RKM simulations, the discretized step has to be manually chosen, and we have checked that solutions only converge for very low values of this variable. Moreover, the optimum choice strongly depends on *T*, so the task becomes a kind of a trial and error game. The BS algorithm due to its adaptive step-size solves this problem, but we have found that the employed computer time becomes larger than with the RKM. Besides, the BS algorithm often fails in calculating the solutions of rather complicated systems of ordinary differential equations.[38] By contrast, Pspice does not face with the problems of the step-size control, due to its adaptive character and the choice of a suitable numerical algorithm to solve the equations. Once the electric analogy of the system has been established with the NSM, it is only necessary to execute the program, without taking into account any programming feature.

Apart from all these considerations, the main feature of Pspice is its speed of execution. Even at low temperatures, where the switching point takes longer to be reached, this software employs a CPU time in the order of seconds. For example, at T=350 K the switching time is approximately equal to 10^{10} s (see Figure 11). By comparing algorithms executed in the same CPU (Intel Core i5, 2.7GHz), standard RKM needs CPU times up to four days to properly reach the switch, while NSM in Pspice employs no more than 10 seconds.

We can summarize the important advantages of the network simulation method, in comparison with other "classical" numerical methods: (i) no mathematical manipulation of the differential equations is needed to solve the problem once the network model is designed; (ii) since the simulation code assumes Kirchhoff´s law of current, the balance of the flow variables (conservation law) is inherently assured without adding new requirements to the model; (iii) very few devices are required to design the equivalent electric network; (iv) the method can be easily extended to other complex systems described by a set of differential equations, so it can be considered as a general approach; (v) the CPU times are very short.

V. Conclusions

The Network Simulation Method, a numerical approach based on the electric analogy of the transport processes, has been successfully employed through its implementation in Pspice, to solve a complex kinetic system. In this way, a set of differential equations, corresponding to the mechanistic paths of a tandem of pericyclic reactions, have been solved, and its kinetic-thermodynamic switching point has been located. These kinetic schemes are usually very difficult to solve analytically without approximations, which do not allow to know in an exhaustive manner the behavior of the solutions over the entire time domain.

To achieve a deeper comprehension of the switching phenomenon, the dependence of the switching time on the reaction temperature has been established, demonstrating that is time, not temperature, the variable fundamentally controlling the kinetic-thermodynamic switch. To the best of our knowledge no previous studies have calculated the kinetic-thermodynamic switching time at different temperatures. When the switching point takes place at long times, these kinds of kinetic studies become unaffordable in practice by employing standard numerical algorithms, because the computational times required grow very fast as the temperature decreases.

In addition, this approach also allows knowing quantitatively the evolution of the concentrations of all participant species along the time, the reaction yield as a function of the reaction time, as well as when the stationary state will be reached. All these predictions let to manage a deep control over the reaction products that could be applied for synthetic purposes without laborious and expensive experimental trials.

In summary, an efficient and very fast procedure has been used for locating the kinetic-thermodynamic switching point of a tandem of pericyclic reactions. It can be applicable to other complex kinetic schemes, which must be previously scrutinized by computational methods for extracting the energy barriers of their individual reactions steps.

Acknowledgements

Part of this work was supported by the Ministerio de Ciencia e Innovacion of Spain (Project No. CTQ2008-05827/BQU) and the Fundacion Seneca-CARM (Project No. 08661/PI/08).

The authors also want to thank University Centre of Defence, at the Spanish Air Force Academy, Base Aerea de San Javier, Murcia, Spain.

Notes and References

[a] University Centre of Defence at the Spanish Air Force Academy, Base Aerea de San Javier, C/Coronel Lopez Peña s/n, Santiago de la Ribera, 30720, Murcia, Spain. Fax: 34 968189970, Tel: 34 968 189974; E-mail, P. Sanchez-Andrada: pilar.sanchez@cud.upct.es; andrada@um.es; M. Caravaca: manuel.caravaca.upct@hotmail.es; A. Soto: antonio.soto@cud.upct.es

[b] Departamento de Quimica Organica, Universidad de Murcia, Facultad de Quimica, Regional Campus of International Excellence "Campus Mare Nostrum", Espinardo, 30100 Murcia, Spain. Tel:34 868887497 E-mail, M. Alajarin: alajarin@um.es

† Electronic Supplementary Information (ESI) available: Figure S1: Stationary regime for concentrations [*cis*-**2a**] and [*trans*-**2a**]; Figure S2: Concentrations of the intermediates, [*Z,Z*-**INTa**], [*E,Z*-**INTa**], [*Z,E*-**INTa**], and [*E,Z*-**INTa**] as a function of the reaction time ; Figure S3: Asymptotic behavior of the ratio [*cis*-**2a**] / [*trans*-**2a**]; Figure S4: Concentration of species **1a** vs time; Figure S5: Asymptotic behavior of the reaction yield. Table S1: Electronic and free energies, relative electronic and free energies of the stationary points found in the transformation **1a** → *cis*-**2a** and *trans*-**2a**; Table S2: Relative free energies computed at different temperatures for the stationary points

found in the transformation **1a** → *cis*-**2a** and *trans*-**2a**; Table S3: Free energy barriers calculated at different temperatures for the individual steps involved in the transformation of **1a** into *cis*-**2a** and *trans*-**2a**; Table S4: Rate constants calculated at different temperatures for the individual steps involved in the transformation **1a** → *cis*-**2a** and *trans*-**2a** computed at the B3LYP/6-31+G** theoretical level. Mathematical treatment of the NSM applied to chemical reactions. See DOI: 10.1039/b000000x/

‡ The authors have developed a software called SimKinet that automatically implements the NSM equivalence between a chemical process and the corresponding electric network, and performs in a friendly-user way the simulation in Pspice to solve the corresponding kinetic study.[39] SimKinet can be downloaded free of charge, by permission, from http://www.ideatic.net/static/SimKinet.zip. ©08/2014/259.

1 [a] E. L. Eliel, S. H. Wilen, In *Stereochemistry of Organic Compounds*, Wiley: New York, 2008. [b] F. A. Carey, R. J. Sundberg, In *Advanced Organic Chemistry: Part A: Structure and Mechanisms*, Springer: New York, 2007. [c] J. Gilbert, S. Martin, In *Experimental Organic Chemistry: A Miniscale and Microscale Approach*, Cengage learning: Boston, 2011.

2 A. Bruggink, E. C. Roos, E. Vroom, *Org. Proc. Res. Develop*. **1998**, *2*, 128-133

3 A. Nagaki, H.Kim, J. Yoshida, *Angew. Chem., Int. Ed. Engl*. **2009**, *48*, 8063-8065.

4 At the best of our knowledge, we have only found a reference where this concept has a proper name, in which is referred as crossing point, see A.Neuforth, P. G. Seybolg, L. B. Kier, C.-K. Cheng, *Int. J. Chem. Kinet*. **2000**, *323*, 529-534.

5 A reviewer has opportunely suggested that for two parallel reactions, where **A** and **B** are the products of kinetic and thermodynamic control, the intersection of dependences of their concentrations can be mathematically considered as a fingerprint, see: [a] G. S. Yablonsky, D. Constales, G. Marin, *Chem. Eng. Sci*. **2010**, 65, 2325-2332. [b] D. Constales, G.S. Yablonsky, G.B. Marin, *Comput. Math. Appl.* **2013**, 65, 1614-1624. In these articles it has been recognized that the intersection points of different concentration curves and the coincidences of such intersections in time constitutes a rich source of transient kinetic fingerprints. Certainly, even though from the mathematical aspect this point could be considered just as a fingerprint, from the chemical one, and in accordance with the definition that we have proposed for the kinetic-thermodynamic switching point, this constitutes a fundamental topic, whose location and characterization would allow to take control over the products composition along time.

6 [a] D. G. Truhlar, B. C. Garrett, S. J. Klippenstein, *J. Phys. Chem*. **1996**, *100*, 12771-12800. [b] K. Laidler, C. King, *J. Phys. Chem*. **1983**, *87*, 2657-2664; [c] D. G. Truhlar, W. L. Hase, J. T. Hynes, *J. Phys. Chem*. **1983**, *87*, 2664-2682. [d] K. J. Laidler, In *Theories of Chemical Reaction Rates*; McGraw-Hill Series in Advanced Chemistry: New York, 1969; pp 234. [e] M. G. Evans, M. Polanyi, *Trans. Faraday Soc*., **1937**, *33*, 448-452. [f] H. Eyring, M. Polanyi, *Z. Phys. Chem. Abt. B*, **1931**, *12*, 279-311. [g] H. Eyring, *J. Chem. Phys*. **1935**, *3*, 107-115.

7 [a] J. Bertran, J. Núñez, In *Quimica Fisica, vol 2*; Ariel: Barcelona, 2002. [b] E. V. Anslyn, D. A. Dougherty, In *Modern Physical Organic Chemistry*; University Science Books: California, 2006; pp 365-373.

8 Between the common approaches, the steady-state approximation is one of the most used since it simplifies notably the calculations. Nevertheless, as in the rest of approximations, it is mandatory to know its interval of validity, and hence a thorough understanding of the kinetic frame where it will be applied. See [a] T. Turanyi, A. S. Tomlin, M. J. Pilling, *J. Phys. Chem*. **1993**, *97*, 163-172. [b] A. R. Tzafriri, E. R. Edelman, *J. Theor. Biol*. **2005**, 343-350. [c] V.Viossat, R. L. Ben-Aim, *J. Chem. Educ*. **1993**, *70*, 732-738.

9 See for example: D. T. Gillespie, *J. Comput. Phys*. **1976**, *22*, 403-434; *J. Phys. Chem*. **1977**, *81*, 2340-2361.

10 Gonzalez-Fernandez, C. F.; Alhama, F.; Horno, J.; Lopez-Garcia, J. J. In *Network Simulation Method*; Research Singpost: Trivandrum, 2002.

11 PSPICE 6.0, 1994. Microsim Corporation Fairbanks, Irvine, California.

12 W. H. Press, S. ATeukolsky, W. T. Vetterlin, B. P. Flannery, In *Numerical Recipes. The art of scientific computing*; Cambridge University Press: New York, 2007.

13 [a] L. Peusner, The principles of network thermodynamics and biophysical applications, PhD Thesis, Harvard University, Cambridge, MA, 1970 [Reprinted by Entropy, Lincoln, MA, 1987]. [b] L. Peusner, *J. Chem. Phys*. **1982**, *77*, 5500-5507. [c] L. Peusner, In *Chemical Applications of Topology and Graph Theory*, Elsevier, Amsterdam, 1983.

14 [a] J. Zueco, A. Campo, *Appl. Therm. Eng.* **2006**, *26*, 673–679. [b] F. Alhama, C. F. Gonzalez-Fernandez, *Heat Mass Transfer*, **2002**, *38*, 327-335.

15 [a] C. F. Gonzalez-Fernandez, M. T. García-Hernandez, J. Horno, *J. Electroanal. Chem*. **1995**, *395*, 39-44. [b] J. Horno, C. F. Gonzalez-Fernandez, A. Hayas. *J. Comp. Phys*. **1995**, *118*, 310-319.

16 A. Soto, F. Alhama, C. F. Gonzalez-Fernandez, *J. Hydrol*. **2007**, *339*, 39-53,

17 [a] F. Alhama, J. Zueco, C. F. Gonzalez-Fernandez *Int. Commun. Heat Mass Transfer*, **2004**, *31*, 929-937. [b] J. Zueco, F. Alhama, C. F. Gonzalez-Fernandez, *Heat Mass Transfer*, **2005**, *41*, 411-418.

18 J. F. Lopez-Sanchez, F. Alhama, C. F. Gonzalez-Fernandez, *Ecol. Modell*. **2005**, *183*, 1-9.

19 E. Castro, M. T. Garcia-Hernandez, A. Gallego, *J. Sound Vib*. **2005**, *283*, 997-1013.

20 [a] R. L. Seither, D. F.Trent, D. C. Mikulecky, T. J. Rape, I. D. Goldman, *J. Biol. Chem*. **1989**, *264*, 17016-23. [b] R. L. Seither, D. Hearne, D. Trent, D. C. Mikulecky, I. D. Goldman, *Computer Math. Applic.* **1990**, *4-6*, 87-101.

21 [a] D. C. Mikulecky, *Comput. Chem*. **2001**, *25* 369-391. [b] A. N. Gorban, O. Radulescu, A. Y. Zinovyev, *Chem. Eng. Sci.* **2010**, *65*, 2310-2324. [c] P. Zupanovic, D. Juretic, *Croat. Chem. Acta* **2004**, *77*, 561-571. [d] A. Shahmoon, Z. Zalevsky, *Processes* **2013**, *1*, 12-29. [e] S. Mandal, R. Sarpeshkar, *IEEE International Symposium on Circuits and Systems ISCAS* **2009**, 2697-2700.

22 L. W. Nagel, SPICE 2. A Computer program to simulate semiconductor circuits. PhD Thesis, University of California, May 1975. http://www.eecs.berkeley.edu/Pubs/TechRpts/1975/9602.html

23 Actually, the occurrence or not of the kinetic-thermodynamic switching point in a chemical reaction leading to two different products depends on the values of the rate constants corresponding to the individual steps, which in turns depends on the relative values of energy barriers associated to those steps. Therefore, two scenarios may be present for a parallel reaction as **A** ⇄ **R** ⇄ **B**, one where the switching point appears, and another with not switching point, in which one of the products should be both the kinetic and thermodynamic controlled product along overall reaction time.

24 [a] L. King-Chuen, *J. Chem. Ed.* **1988**, *65*, 857-860. [b] F. A. Matsen, J. L. Franklin, *J. Am. Chem. Soc*. **1950**, *72*, 3337-3341.

25 M. Alajarin, B. Bonillo, M. Marin-Luna, P. Sanchez-Andrada, A. Vidal, R.-A. Orenes *Tetrahedron* **2012**, *68*, 4672-4681.

26 For similar kinetic studies, involving different kind of processes, which we have previously accomplished see for example: [a] M. Alajarin, A. Vidal, F. Tovar, A. Arrieta, B. Lecea, F. P. Cossio, *Chem. Eur. J*. **1999**, *5*, 1106-1117. [b] F. P. Cossio, A. Arrieta, M. Alajarin, A. Vidal, F. Tovar, *J. Org. Chem.* **2001**, *65*, 3633-3643 [c] M. Alajarin, P. Sanchez-Andrada, A. Vidal, F. Tovar, *J. Org. Chem*. **2005**, *70*, 1340-1349. [d] M. Alajarin, P. Sanchez-Andrada, A. Vidal, F. Tovar, *J. Org. Chem*. **2004**, 2636-2643.

27 See reference 25 and the associated supporting info.

28 Besides, we had an experimental proof indicative of the obtained diasteroemeric ratio was the result of the kinetic control of the reaction. See reference 25.

29 According to eqs. (19)-(22) the concentrations of *cis*-**2a** and *trans*-**2a** are time dependent, but the ratio [*cis*-**2a**] / [*trans*-**2a**] is not time dependent.

30 M. J. Frisch, G. W. Trucks, H. B. Schlegel, G. E. Scuseria, M. A. Robb, J. R. Cheeseman, G. Scalmani, V. Barone, B. Mennucci, G. A. Petersson, H. Nakatsuji, M. Caricato, X. Li, H. P. Hratchian, A. F. Izmaylov, J. Bloino, G. Zheng, J. L. Sonnenberg, M. Hada, M. Ehara, K. Toyota, R. Fukuda, J. Hasegawa, M. Ishida, T. Nakajima, Y. Honda, O. Kitao, H. Nakai, T. Vreven, J. A. Montgomery, Jr., J. E. Peralta, F. Ogliaro, M. Bearpark, J. J. Heyd, E. Brothers, K. N. Kudin, V. N. Staroverov, R. Kobayashi, J. Normand, K. Raghavachari, A. Rendell, J. C. Burant, S. S. Iyengar, J. Tomasi, M. Cossi, N. Rega, J. M. Millam, M. Klene, J. E. Knox, J. B. Cross, V. Bakken, C. Adamo, J. Jaramillo, R. Gomperts, R. E. Stratmann, O. Yazyev, A. J. Austin, R. Cammi, C. Pomelli, J. W. Ochterski, R. L. Martin, K. Morokuma, V. G. Zakrzewski, G. A. Voth, P. Salvador, J. J. Dannenberg, S. Dapprich, A. D. Daniels, O. Farkas, J. B. Foresman, J. V. Ortiz, J. Cioslowski, and D. J. Fox, Gaussian, Inc., Wallingford CT, 2009.

31 Variable time on Figure 6 ranges from 0 to $1.0 \cdot 10^8$ s in order to clearly show the switching point. The time required to raise the stationary state for all curves is shown in Figure S1 of the Supporting Information.

32 The asymptotic behavior of the ratio [*cis*-**2a**]/[*trans*-**2a**] is shown in Figure S3 of the Supporting Information.

33 We have computed the reaction yield through the following expression, which defines the so called molar yield: Molar Yield (t) (%) = 100 x ($[cis\text{-}\mathbf{2a}]_t$ + $[trans\text{-}\mathbf{2a}]_t$)/ $[1a]_0$, where $[cis\text{-}\mathbf{2a}]_t$ and $[trans\text{-}\mathbf{2a}]_t$ are the concentration of the species **1a**, *cis*-**2a**, and *trans*-**2a** at a time t (note that the transformation of **1a** into *cis*-**2a** + *trans*-**2a** is an intramolecular reaction).

34 As mentioned above, the rate constants have been calculated from equation 10, $k_i = \frac{k_B \cdot T}{h} \cdot e^{-\frac{\Delta G_i}{RT}}$, according to the transition state theory. From this equation it can be easily recognized that rate constants present a strong dependence on T.

35 R. B. Snadden, *J. Chem. Ed*. **1985**, *62*, 653-655.

36 P. L. DeVries, J. E. Hasbun, In *A First Course in Computational Physics*; Jones and Barlett Publishers, LLC, 2011.

37 Gustafsson, K., *ACM Trans. Math. Softw*. **1994**, *20*, 496-517.

38 A. W. Neumann, R. David, Y. Zuo, In *Applied Surface Thermodynamics*; CRC Press, 2010.

39 Several computer software packages for modelling complex kinetic schemes are commercially available. The ChemKin Collection is a very popular one, mostly used in combustion, catalysis, corrosion, plasma etching and chemical vapor deposition, among other applications. However, its use is not simple enough but it request previous training. The SimKinet software, developed by the authors, is probably simpler than any commercial software for kinetic applications, it is completely free, it has a very user-friendly interface and it does not even require in-home installation. The user must basically enter the differential equations and the kinetic rate constants, without any further manipulation. Besides, as stated in the main text, SimKinet is orders of magnitude faster than other numerical methods for solving differential equations.

TOC GRAPHIC

Fast and effective location of the switch point between kinetic and thermodynamic regimes by means of the NSM approach provides a comprehensive control over the product composition